REMOTELY SENSED L-BAND SAR DATA FOR TROPICAL FOREST BIOMASS ESTIMATION

O Hamdan*, H Khali Aziz & K Abd Rahman

Forest Research Institute Malaysia, 52109 Kepong, Selangor Darul Ehsan, Malaysia

Received September 2010

HAMDAN O, KHALI AZIZ H & ABD RAHMAN K. 2011. Remotely sensed L-band SAR data for tropical forest biomass estimation. Several attempts have been made to obtain forest stand parameters such as stand volume, stand density, basal area, biomass and carbon (C) stocks from synthetic aperture radar (SAR) data. However the relationship between these parameters and radar backscatter has been a challenging issue since the last several years. In this study, L-band ALOS PALSAR satellite image with a spatial resolution of 12.0 m was utilised to identify the relationship between radar backscatter and aboveground biomass of tropical forest stands. Forest Research Institute Malaysia (FRIM) which has about 420 ha of forest area was selected as the study area. Field survey was conducted in which 30 plots (50 × 50 m, 0.25 ha each) were established and all trees with diameters at breast height (dbh) of 5 cm and above were inventoried. The calculated plot-based biomass was correlated to the pixels of SAR backscatter corresponding to the plot size on the ground. The correlation function was used to determine stand biomass of the whole study area. Results showed that dense forest was sensitive to the backscatter on horizontal–vertical polarised (HV) image compared with horizontal–horizontal polarised (HH) image. It was also found that the L-band SAR backscatter had good capability to estimate aboveground biomass in mature stands of tropical forest.

Keywords: ALOS PALSAR, SAR backscatter, stand biomass, aboveground biomass

HAMDAN O, KHALI AZIZ H & ABD RAHMAN K. 2011. Data penderiaan jauh SAR jalur-L untuk penilaian biojisim hutan tropika. Beberapa percubaan telah dibuat untuk mendapatkan parameter dirian hutan seperti isi padu dirian, kepadatan dirian, luas pangkal pokok, biojisim dan stok karbon daripada data radar bukaan sintetik (SAR). Bagaimanapun, hubungan antara parameter-parameter tersebut dengan serak balik radar merupakan isu yang mencabar sejak beberapa tahun lalu. Dalam kajian ini, imej satelit ALOS PALSAR yang berjalur-L dengan resolusi ruang 12.0 m telah diguna untuk mengenal pasti hubungan antara serak balik radar dengan biojisim atas tanah bagi dirian hutan tropika. Institut Penyelidikan Perhutanan Malaysia (FRIM) yang mempunyai 420 ha kawasan berhutan telah dipilih sebagai kawasan kajian. Bagi tujuan ini, 30 plot setiap satunya bersaiz 50 m × 50 m (0.25 ha) telah ditubuhkan dan kesemua pokok yang mempunyai saiz diameter aras dada (dbh) 5 cm dan ke atas telah dibanci. Biojisim bagi setiap plot telah dikira dan dikaitkan dengan nilai piksel serak balik data SAR yang bersesuaian dengan saiz plot di lapangan. Persamaan yang terbit daripada hubungan tersebut diguna untuk menentukan biojisim bagi keseluruhan dirian di dalam kawasan kajian. Hasil kajian menunjukkan bahawa hutan yang berkepadatan tinggi lebih sensitif terhadap imej yang berpolar mengufuk–vertikal berbanding imej yang berpolar mengufuk–mengufuk. Didapati juga bahawa serak balik radar berjalur-L mempunyai keupayaan yang baik untuk menganggar biojisim atas tanah bagi dirian hutan tropika matang.

INTRODUCTION

Forests only cover 28% of the land surface worldwide but contain 80% of the terrestrial carbon (C), stored as biomass and soil organic C (FAO 2005). Tropical forests are a key component of the global C cycle and contribute more than 30% of terrestrial C stocks and net primary production (Wright 2010). However, at the same time tropical deforestation contributes about one fifth of total anthropogenic CO_2 emissions to the atmosphere (Gibbs et al. 2007). In global environment and climate studies, forest biomass is a key variable in annual and long-term changes in the terrestrial C cycle, and is needed in modelling C uptake and redistribution within the ecosystem (Houghton 2005). However the estimations of global terrestrial biomass remain uncertain and are still being studied in line with the understanding of global C cycle.

The suggested schemes for C credit allocation based on deforestation or C stock baselines require accurate estimates of biomass. Forest biomass can be evaluated using remote sensing

**E-mail: hamdanomar@frim.gov.my*

instruments mounted on satellites or airborne platforms, but substantial refinements are needed before routine assessments can be made at national or regional scales (Baccini et al. 2004, DeFries et al. 2007). There are no remote sensing instruments that can measure forest biomass directly, thus, additional ground-based data collection is required (Drake et al. 2003, Rosenqvist et al. 2003a). A satellite-based approach can provide the spatial pattern of observation needed for biomass at a landscape level.

For systematic observation at different scales, remote sensing is considered a major component of forest monitoring programmes (Lu 2006). The focus to date, however, has mainly been on the use of optical data (Toan et al. 2001, Miettinen & Liew 2009). Remote sensing systems that mostly rely on optical data (visible and infrared light) are further limited in the tropics by cloud cover (Asner 2001). Meanwhile, research results indicate that synthetic aperture radar (SAR) has a significant role to play in forest observations (Chenli et al. 2005).

The interest in radar remote sensing for monitoring forest cover rose from the two advantages of SAR data, namely, (1) radar can provide information related to the canopy volume which cannot be produced by other means and (2) radar has the possibility of acquiring data over areas with frequent cloud cover and not depending on weather conditions. The information that can be derived from SAR data includes aboveground biomass, annual increment of stand biomass, vertical distribution of biomass and forest stand volume. Refining these estimates requires improved knowledge of the densities and spatial distribution of forest C stocks, particularly in high biomass tropical forest ecosystems.

Remote sensing methodologies are more successful at measuring aboveground biomass in boreal and temperate forests and in young stand with lower biomass density (Austin et al. 2003, Rosenqvist et al. 2003b) compared with dense and mature stands. Tropical forests are among the most biomass- and C-rich but are the most structurally complex ecosystems in the world that most signals from remote sensing instruments tend to saturate at certain biomass level. Short wavelength SAR sensors on board several satellites such as Earth Resources Satellite (ERS-1), Japanese Earth Resources Satellite (JERS-1) and Environmental Satellite (Envisat) can be used to quantify forest biomass in relatively homogeneous or young forests, but the signal tends to saturate at fairly low biomass levels (100–200 t ha^{-1}) (Patenaude et al. 2004, Toan et al. 2004, Chenli et al. 2005). Actually, there is potential to improve estimates of biomass across the tropics for degraded or young forests but will be less useful for mature, higher biomass forests (Rosenqvist et al. 2003b, Shimada et al. 2005).

Phased Array L-band SAR (PALSAR) on board the Japanese Advanced Land Observing Satellite (ALOS), however, promises better potential in assessing forest biomass for tropical ecosystem (Baccini et al. 2008). Thus, it has produced reliable forest biomass estimates in this ecosystem. Remote sensing offers the possibility of providing relatively accurate forest biomass estimation at a lower cost than inventory studies in tropical forests; L-band JERS-1 SAR has been successfully used in the Malaysian tropical inland and peat swamp forests (Khali Aziz 2000). SAR is known to have a response that is directly related to the amount of living material with which it interacts. The radar backscatter obtained from SAR is proportional to vegetation density up to a saturation point that is dependent upon wavelength and polarisation of the radar.

There are numerous biomass estimation models that have been published in the literature. The models vary basically with respect to the characterisation of forest and the calculation of its scattering properties. The interaction of SAR signals with the forest is dependent on the radar wavelength and the stand structure of the forest itself. The frequency of SAR is directly proportional to the depth of wave penetration, which means that shorter wavelength can only penetrate the forest for a few centimetres, while longer wavelength can penetrate deeper and sometimes can interact with the forest floor (Imhoff 1995). Tree elements that play a major role in the scattering and attenuation at different frequency bands are summarised in Table 1. However, the relative contribution of different components may change with the tree species and their development state. Likewise, at a given frequency, the scattering and attenuation sources can change with the polarisation and incidence angle.

Some SAR systems have the capability to send and receive energy with different polarisations. Since SAR energy can be depolarised upon interaction with various surface features, independently recording the reflection of like-

Table 1 Tree elements which are the main scatterers at different radar bands or wavelengths

Radar band	X	C	L	P
Wavelength (cm)	2.4–3.75	3.75–7.5	15–30	30–100
Main scatterers	Leaves, twigs	Leaves, small branches	Branches, trunks	Trunks

polarised energy (e.g. vertical send–vertical receive (VV) or horizontal send–horizontal receive (HH)) and cross-polarised energy (e.g. vertical send–horizontal receive (VH) or horizontal send–vertical receive (HV)) can yield valuable information regarding the characteristics of imaged features, and can be particularly useful in the analysis of vegetation type and structure. ALOS PALSAR has two polaristions, HV and HH, which allows polarisation selection.

Currently, there is no comprehensive study that uses PALSAR data to map spatial distribution of aboveground forest biomass and C stocks in Malaysia. Therefore, this study was carried out to (1) establish empirical relationship between aboveground biomass and PALSAR signals for tropical forest ecosystem, (2) determine aboveground biomass by using L-band SAR data, and (3) identify the capability of ALOS PALSAR satellite imagery in estimating aboveground biomass.

MATERIALS AND METHODS

Study area

The Forest Research Institute Malaysia (FRIM) at Kepong, Selangor was selected as the study area. With an area of about 485.2 ha, FRIM is surrounded by the Bukit Lagong Forest Reserve. Of the total area, 420.11 ha are covered by forest, of which 379.98 ha are planted forest comprising mostly lowland and hill dipterocarp trees species. The remaining 40.12 ha are natural forest. Most of the trees planted here are about 80 years old (planted since year 1929). Newly planted trees are also included in the field data collection and plot sampling in this study. Figure 1 shows the location of study area, marked with a black square.

Satellite data

ALOS, an enhanced successor of the JERS-1, was launched from JAXA's Tanegashima Space Center in January 2006. ALOS operates from a sun-synchronous orbit at 691 km, with a 46-day recurrence cycle carrying a payload of three remote sensing instruments: (1) the Panchromatic Remote Sensing Instrument for Stereo Mapping (PRISM), (2) the Advanced Visible and Near-Infrared Radiometer type 2 (AVNIR-2) and (3) the polarimetric Phased Array L-band SAR (PALSAR). ALOS PALSAR image that was used in this study was acquired on 3rd October 2009. The image came with two polarisations, horizontal–horizontal (HH) and horizontal–vertical (HV) and has spatial resolution of 12 m.

Field inventory data

Field inventory was launched on 22 January 2010 and 30 sampling plots of 50 × 50 m size were established within the study area (Figure 2). The plots cover both types of forests, i.e. natural and planted forests at various ages. Square plot design was used in this study to facilitate pixel sampling on any satellite imagery, reduce position error caused by Global Positioning System (GPS) observation, and make the orientation similar to the shape of the satellite image pixel, which is normally square. By recording the coordinate of the location only at the centre of the plots (instead of each square edge), position accuracy was improved. The plot could also be located precisely on the satellite image. By following this approach, sampling error caused by plot displacement was minimised. While observing the central coordinate, bearing and distances from the central to the quadrate directions were measured using prismatic compass and distance tape respectively. Systematic sampling design was applied for the purpose of field sampling in which selection of sampling plots was based on forest types and ages. Of the 30 sampling plots established, 70% were inside the mature stand forest (of ages more than 50 years) and the rest were distributed within 5- to 30-year-old stands.

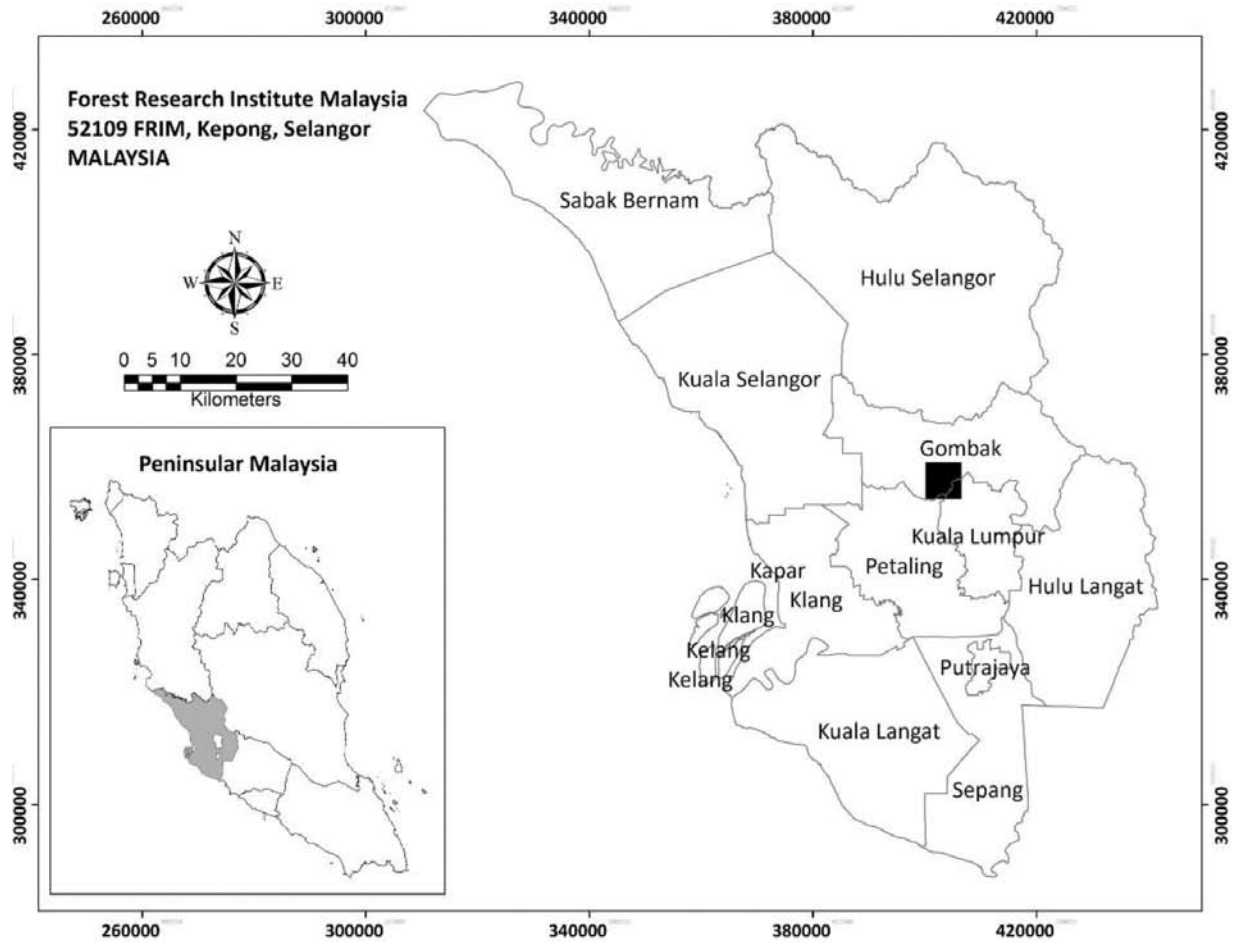

Figure 1 Location of the study area

Most of the trees in the study plots are above 25 m height and reach up to 45 m, with canopy closure of more than 85% especially for the kapur (*Dryobalanops aromatica*) trees. These kinds of stands contributed substantially to the level of biomass at specific points and thus introduce variations in the measured biomass in the study area. Associated information such as tree height was also recorded where possible using a laser hypsometer. The dominant species of standing trees within each plot was also recorded. Most inventories only include trees with diameters at breast height (dbh) ≥ 10 cm but according to Chave et al. (2005) and Baccini et al. (2008), about 25% of the total aboveground biomass will be missed out if the trees with dbh of 5 cm are not included, which will produce underestimate. Therefore, all trees with the size of dbh ≥ 5 cm were inventoried in this study.

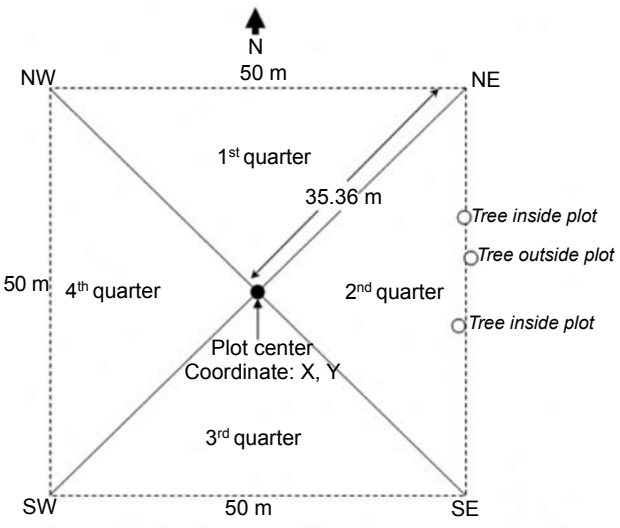

Figure 2 Layout design of the sampling plot

Plot level biomass estimation

A tree is made up of several biomass components, namely, foliage, stem, stump, root, bark and branch. The proportion of these components varies with tree species and tree age. While young trees have rather high biomass proportions of leaves/needles and roots, old trees have a high proportion of stem biomass. Conversion factors or allometric equation do not provide

information on biomass components accurately unless they are validated for the species, age and site under consideration. In Malaysia, biomass equations have been developed for the inland forest based on destructive sampling (Kato et al. 1978). The allometric function of trees applied in the calculation of standing biomass can be expressed as in equation 1. The key parameter is dbh.

$$1/H = 1/(2.0 \times D)+1/61 \quad (1)$$

where H = total tree height and D = dbh. From the values of D and H, the dry mass values of stem (M_s), branches (M_b) and leaves (M_l) of the tree were estimated.

$$M_s = 0.0313 \times (D^2H)^{0.9733} \quad (2)$$
$$M_b = 0.136 \times M_s^{1.070} \quad (3)$$

$$1/M_l = 1/(0.124M_s^{0.794})+1/125 \quad (4)$$

Therefore, the total aboveground biomass for a tree was the summation of M_s, M_b and M_l. While the total aboveground biomass was calculated on plot basis, the within-plot variations of aboveground biomass for the whole established plots were also analysed. There were about 50 to 250 trees of dbh ≥ 5 cm (range 5–109 cm) found in each plot established. A total of 4833 trees were inventoried and the aboveground biomass of each tree ranged between 0.01 and 16.3 t tree^{-1} (derived from the above equations).

Methodology

The three major steps involved in deriving biomass from ALOS PALSAR satellite image are image pre-processing, plot sampling and aboveground biomass estimation. These processes are explained below.

Image pre-processing

The PALSAR image that was used in this study was supplied by the Remote Sensing Technology Center of Japan (RESTEC), the designated primary distributor of ALOS satellite data. The image was in Level 1.5 format in HV and HH polarisations. It was built on 16-bit data type and all pixels had digital numbers (DNs) ranging from 0–65 535. These DNs, however, did not represent the radar signal of features or objects on the ground. Therefore, the DNs had to be converted to backscatter coefficients (radar signals) known as Normalised Radar Cross Section (NRCS) and represented in decibels (dB). The equation that was used for the calculation of PALSAR NRCS was slightly different from other sensors in that the usual sine term had already been included in the DN values. Thus, for the data stored in Level 1.5 products, the equation for NRSC of any of the polarisation component can be obtained by the following formula with single calibration factor, which can be expressed as equation 5 for distributed scatterers. The conversion factor (CF) used in the equation is valid for data obtained after 9 January 2009 (Shimada et al. 2009).

$$\text{NRCS (dB)} = 10 \times \log_{10}(DN^2) + CF \quad (5)$$

where CF = -83.0

Other than conversion of the DN to NRCS, there are two other pre-possessing stages, namely, speckle suppression and radiometric terrain correction. Spatial domain Lee Sigma filter with a kernel size of 3 × 3 pixels was used to remove speckle effects on the image. Digital Elevation Model (DEM) that was generated from contour lines extracted from topographic map was used to minimise shadows on the image as a result from 'shadowing' effect of the radar backscatter. The presence of this effect on SAR imagery was because the signal strengths were dependent on two variables, which were incidence angle and surface roughness or topography of terrain. If a slope is facing the SAR transmitter, the signal that is transmitted back to the sensor will become stronger than the other side of the slope. Therefore, this process was necessary to normalise both sides of the slope and it minimised errors towards the end of biomass prediction.

Plot sampling and aboveground biomass estimation

Plot sampling process was carried out to extract the NRCS of the satellite image at corresponding locations on the ground. A ground plot with the size of 50 × 50 m can cover about 16 pixels with the dimension of 4 × 4 pixels. An average value of the NRCS within the 16 pixels was used for the correlation. In this case, the NRCS were the predictor or estimator for the measured biomass on the ground. Both signals and total biomass within each plot were correlated to produce a regression function.

Regression analysis is an appropriate statistical technique to study the relationship between two continuous variables such as forest biomass and radar backscatter. In this case, NRCS from both HV- and HH-polarised SAR images were regressed against the measured biomass. It was found that the HV polarisation returned stronger relationship with stand biomass. This correlation has been chosen to derive a prediction equation that was used to quantify aboveground biomass for the whole study area. The relationship between NRCS and aboveground biomass can be expressed as:

$$\text{NRCS (dB)} = 3.9704 \ln(\text{biomass}) - 35.533 \quad (6)$$

Equation 6 can be inverted and rewritten as:

$$\text{Biomass (t ha}^{-1}) = 3110.2 \times e^{0.1946\,(\text{NRCS})} \quad (7)$$

($r^2 = 0.7835$, $p < 0.0001$)

RESULTS AND DISCUSSION

Figure 3 shows the scatter plot that consists of measured biomass and corresponding SAR backscatter from ALOS PALSAR image. It has been reported that at a given polarisation and incidence angle, the saturated backscatter value for forest is within a small range of backscatter, typically between -8 and -11 dB at HH or VV and between -11 and -15 at HV (Toan et al. 2001). The dynamic range is thus primarily determined by the backscatter at low biomass. It increases with decreasing frequency and it is higher at HV polarisation than HH or VV. The HV polarisation of ALOS PALSAR backscattering coefficients for all plots in the study area ranged from -7.8 to -18.0 dB (mean of -13.7 dB). The trend line indicated that the biomass component had a logarithmic correlation with the backscattering coefficient which meant that the higher the biomass the greater the backscatter.

The backscatter at low biomass varied as a function of dielectric and structural properties of the main scatterers. In this concern, the forest medium can be considered as a homogenous medium containing a large number of scatterers of a single category and attenuation is sufficiently important to make the ground scattering negligible. In this case, attenuation and scattering compensate each other and the increase in volume of scatterers (increase in number for a given size or increase in size for a given number) will not change the backscatter value. The saturated backscatter value depends mainly on the orientation, size and dielectric constant distribution of the backscattering and forward scattering functions of the individual scatterer (Chen et al. 2009). SAR backscattering will start to saturate when the aboveground biomass level reaches at 150 t ha^{-1} (Quinones & Hoekman 2004). This means that if the aboveground biomass increases to more than 150 t ha^{-1}, the backscatter will become almost constant. This is similar to what was observed in this study. The normalised radar cross section (or backscatter) increased rapidly as the biomass increased but the sensitivity began to reduce slightly as the biomass exceeded 150 t ha^{-1} (Figure 3).

Biomass distribution in the study area

The total aboveground biomass for primary moist forest in Malaysia is the highest (255–446 t ha^{-1} across 15 inventory subunits in moderate, superior hill forest) compared with Cameroon (238–314 t ha^{-1}), French Guiana (280–283 t ha^{-1} for two inventory subunits) and Sri Lanka (153–221 t ha^{-1}). Aboveground biomass as high as 562.2 t ha^{-1} has been recorded in Bukit Lagong Forest Reserve (Abdul Rashid et al. 2009). A rather high (410 t ha^{-1}) biomass content, almost similar to the forests in Malaysia, was also reported for the rain forest in the eastern Amazon (Mazzei et al. 2010).

The aboveground biomass in the study area ranged from 25.9 to 569.3 t ha^{-1} (Figure 4). The distribution was divided into four categories with respect to the different levels of forest growth (Table 2).

The highest quantities of biomass were found in mature and very dense stands, ranging from 427 to 569 t ha^{-1} and occupying about 4% of the whole study area (Table 2). Higher concentration of biomass was observed because the forest was dominated by huge, tall and mature trees especially since these sites were planted with close plant spacing which made this forest denser than the other areas, natural forest included. This is one of the unique forest characteristics found in the study area. Mature and dense stands had the most area coverage, i.e. about 51%, with biomass ranging from 168 to 414 t ha^{-1}. The trees in this category were within long-term ecological plots and were more than 40 years old. The other two categories, namely, small and growing as well as mixed small and mature stands occupied areas of about 28 and 17% respectively. These categories

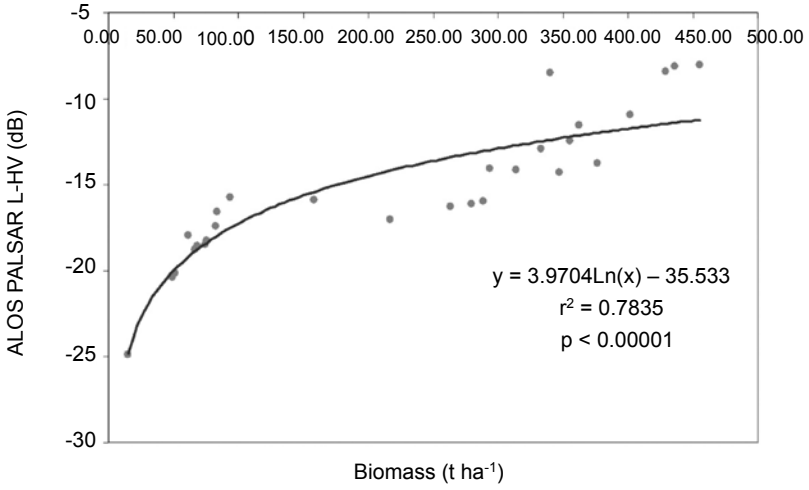

Figure 3 Scatter plot for the correlation of measured aboveground biomass and normalised radar cross section (backscatter, dB)

Table 2 Pattern of biomass distribution in the study area

Category	Range of biomass (t ha^{-1})	Area coverage (%)
Small, growing stands	26–116	28.2
Mixed small, mature stands	130–155	16.9
Mature, dense stands	168–414	51.1
Mature, very dense stands	427–569	3.9

consisted mostly of newly planted trees, 5–30 years old. These categories can also be found spatially distributed in the south-west region of the study area, near Bukit Hari and Kepong Botanical Gardens (Figure 5).

This study demonstrated that L-band ALOS PALSAR data had a positive indicator in estimating aboveground biomass. Results from the correlation that was derived in this study were also encouraging. This proves that L-band SAR data have the capability in assessing forest stands biomass for tropical forest. The aboveground biomass estimation equation is therefore valid for any L-band SAR data.

Validation and verification

In order to validate the results, 11 check plots distributed within the study area were randomly selected. These plots were established independently, specifically for validation process. An absolute accuracy was calculated for the resulted biomass distribution. Absolute accuracy is a measure of error between a derived/predicted biomass from satellite image and the actual biomass measured on the ground. To produce a prediction with good absolute accuracy, reliable ground control (coordinate of the plot centre) can be used to reduce biases. Absolute accuracy (as shown in Table 3) is expressed as the vertical root mean square error (RMSE) of the vertical error measured at geographic coordinates given by

$$\text{RMSE} = \sqrt{\left[\frac{1}{n}\sum_{i=1}^{n}\left((b_i - b_i^{'}) - \mu\right)^2\right]} \qquad (8)$$

where

n = the number of check plots
b_i = measured biomass at check plot i
b_i' = derived/predicted biomass at position i
μ = average of biomass difference

Magnitude of errors of the 11 check plots ranged from -0.1 to -24.25 (Table 3). The huge variations that occurred within the distribution represented the randomness of the check plots. The mean error of -4.77 indicated that the generated biomass from the equation

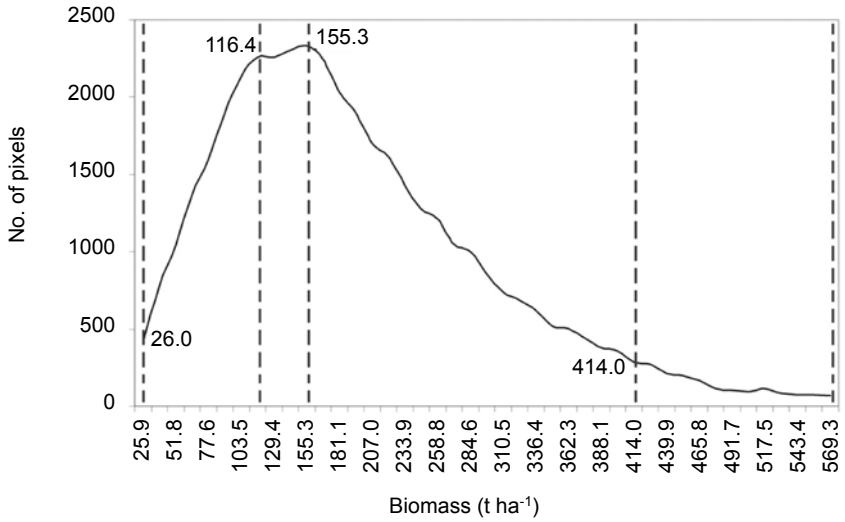

Figure 4 Patterns of distribution of the aboveground biomass in the study area

had underestimated the biomass by about 4.8 t ha^{-1}. Having calculated the RMSE, the biomass within the study area was therefore reported as ranging from 25.9 ± 10.9 to 569.3 ± 10.9 t ha^{-1}, with a mean of 193.6 ± 10.9 t ha^{-1}.

The total biomass within the study area was also calculated based on the distribution of the pixels that represented biomass on the image. Considering biomass in per pixel basis, which was 12 × 12 m, the aboveground biomass within the study area ranged from 0.4 to 8.2 t $pixel^{-1}$ (mean 2.79 t $pixel^{-1}$). From the spatial distribution of the whole pixels, total biomass can be obtained by summing all pixel values. The total aboveground biomass within the study area was 113 749.8 t. The spatial distribution represented by the whole pixels enabled aboveground biomass in the study area to be mapped as shown in Figure 5.

Once biomass has been quantified, C stocks within the study area can be calculated using a conversion factor. As the conversion factor may vary according to plant parts, species and site (Abdul Rashid et al. 2009), the global default conversion factor of 50% was used as recommended by the Intergovernmental Panel on Climate Change (IPCC 2007). Therefore, the total C stocks in the study area were equal to half of the 113 749.8 t of biomass, i.e. 56 874.9 t C; this gave a value of between 12.95 ± 5.45 and 284.65 ± 5.45 t C ha^{-1} (mean 96.80 ± 5.45 t C ha^{-1}).

CONCLUSIONS

The study showed that L-band ALOS PALSAR data had successfully predicted aboveground biomass over all forested areas in this study. The strong correlation between aboveground biomass and radar backscattering coefficient in HV polarisation from ALOS PALSAR image had introduced an alternative for assessing aboveground biomass, which was one of the most important forest stand parameters. Overall, the aboveground biomass values ranged from 25.9 ± 10.9 to 569.3 ± 10.9 t ha^{-1} which covered all types of standing forests in the study area. From this information, a spatially distributed map that showed spatial pattern of aboveground biomass for the whole study area was produced. Aboveground C stocks were between 12.95 ± 5.45 and 284.65 ± 5.45 t C ha^{-1}. Natural and mature standing planted forest showed higher concentration of living biomass compared with some regions with less or sparsely distributed mature, big and tall trees.

Results also indicated that despite its limitations, the use of L-band SAR could provide an alternative for rapid assessment of biomass as well as C stocks in a large area. The technique can be applied to any mature forest areas in the tropical region with similar characteristics, especially in Malaysia. Remote sensing can be used economically to assist the modern management and protection of forest areas. It provides information to facilitate ground-based investigations. The generated information can be used as a guide for preliminary designs in national level biomass assessment. The derived equation is also valid for any tropical forest using L-band SAR data.

With advancements in remote sensing technology and increasing availability of many

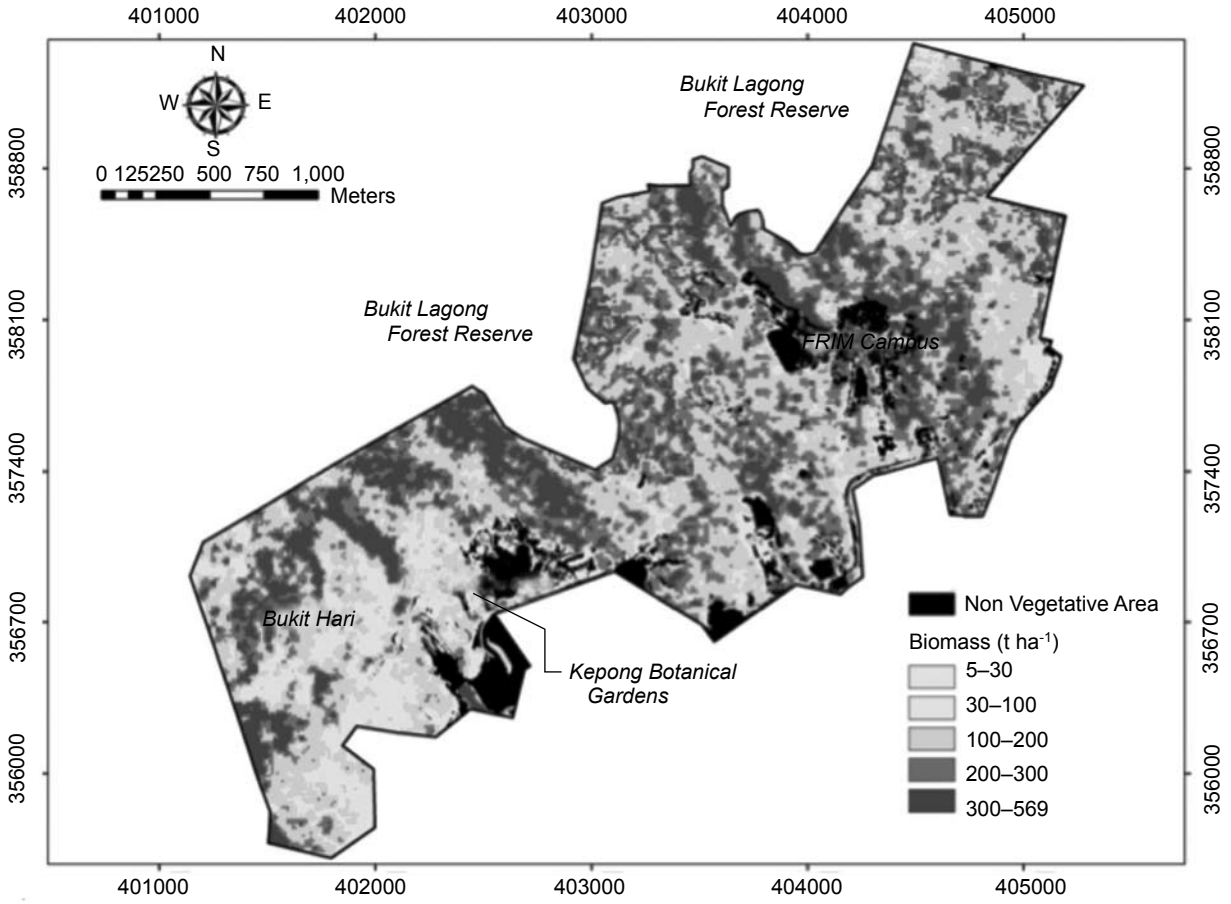

Figure 5 Map showing spatial pattern of aboveground biomass distribution in the study area

Table 3 Absolute accuracy of the predicted biomass

Plot ID	Measured biomass, b (t ha^{-1})	Predicted biomass, b' (t ha^{-1})	Magnitude of error b – b'	Mean square error $((b - b') - \mu)^2$
P 143	411.95	400.79	-11.16	40.77
P 158	368.33	355.20	-13.14	69.84
P 16	366.60	357.03	-9.57	22.93
P 165	130.39	142.29	11.91	278.10
P 179	145.38	145.28	-0.10	21.87
P 213	268.81	258.28	-10.54	33.24
P 231	258.18	253.30	-4.87	0.01
P 250	442.34	458.57	16.23	441.38
P 277	112.88	106.43	-6.45	2.81
P 316	176.74	152.29	-24.45	387.10
P 319	218.65	218.27	-0.39	19.26
			μ = -4.77	RMSE = ±10.9 t/ha

new air- or space-borne satellite systems having fine spatial and spectral resolutions, SAR technology is becoming increasingly suitable for forestry studies that can support decision making to ensure sustainable forest management practices

ACKNOWLEDGEMENTS

The authors would like to thank the Malaysian Forestry Research and Development Board for providing the fund for this study through the Research and Pre-Commercialisation Grant.

Thanks also go to all staff of the Remote Sensing and GIS Branch, FRIM for their support during field survey.

REFERENCES

Abdul Rashid AM, Shamsudin I, Ismail P & Fletcher SC. 2009. *The Role of FRIM in Addressing Climate-Change Issues*. Research Pamphlet No. 128. Forest Research Institute Malaysia, Kepong.

Asner GP. 2001. Cloud cover in Landsat observations of the Brazilian Amazon. *International Journal of Remote Sensing* 22: 3855–3862.

Austin JM, Mackey BG & Van Niel KP. 2003. Estimating forest biomass using satellite radar: an exploratory study in a temperate Australian *Eucalyptus* forest. *Forest Ecology and Management* 176: 575–583.

Baccini A, Friedl AMA, Woodcock CE & Warbington R. 2004. Forest biomass estimation over regional scales using multisource data. *Geophysical Research Letter* 31: L10501.

Baccini A, Laporte N, Goetz SJ, Sun M & Dong H. 2008. A first map of tropical Africa's above-ground biomass derived from satellite imagery. *Environmental Research Letter* 3: 9 pp.

Chave J, Andalo C, Brown S, Cairns MA, Chambers JQ, Eamus D, FoLster H, Fromard F, Higuchi N, Kira T, Lescure JP, Nelson BW, Ogawa H, Puig H, Rie´Ra B & Yamakura T. 2005. Tree allometry and improved estimation of carbon stocks and balance in tropical forests. *Ecosystem Ecology* 145: 87–99.

Chen E, Li Z, Ling F, Lu Y, He Q & Fan F. 2009. Forest volume density estimation capability of Alos Palsar data over hilly region. *Proceedings of the International Workshop on Science and Applications of SAR Polarimetry and Polarimetric Interferometry, PollnSAR*. 26–30 January 2009, Frascati.

Chenli W, Zheng N, Xiaoping G, Zhixing G & Pifu C. 2005. Tropical forest plantation biomass estimation using RADARSAT-SAR and TM Data of South China. Pp 61–69 in Liangpei Z, Jianqing Z & Mingsheng L (Eds) *Proceedings of the Fourth International Symposium on Multispectral Image Processing and Pattern Recognition (MIPPR)*. 31 October–2 November 2005, Wuhan.

DeFries R, Achard F, Brown S, Herold M, Murdiyarso D, Schmlamadinger B & deSouza C. 2007. Earth observations for estimating greenhouse gas emissions from deforestation in developing countries. *Environmental Science Policy* 10: 385–394.

Drake JB, Knox RG, Dubayah RO, Clark DB, Condit R, Blair JB & Hofton M. 2003. Above-ground biomass estimation in closed-canopy neotropical forests using lidar remote sensing: factors affecting the generality of relationships. *Global Ecological Biogeography* 12: 147–159.

FAO. 2005. *State of the World's Forest*. Food and Agriculture Organization of the United Nations, Rome.

Gibbs HK, Brown S, O'Niles J & Foley JA. 2007. Monitoring and estimating tropical forest carbon stocks: making REDD a reality. *Environmental Research Letter* 2: 13 pp.

Houghton RA. 2005. Tropical deforestation as a source of greenhouse gas emissions. In *Tropical Deforestation and Climate Change*. Instituto de Pesquisa Ambiental Amazônia (IPAM), Belém.

Imhoff ML. 1995. A theoretical analysis of the effect of forest structure on synthetic aperture radar backscatter and the remote sensing of biomass. *IEEE Transactions on Geoscience and Remote Sensing* 33: 341–352.

IPCC. 2007. *Climate Change 2007: Synthesis Report. Contribution of Working Group I, II and III to the Fourth Assessment Report of the Intergovernmental Panel on Climate Change*. IPCC, Geneva.

Khali Aziz H. 2000. JERS-1 SAR backscatter characteristics of tropical peat swamp forest. *Malaysian Journal of Remote Sensing* 1: 1–12.

Kato R, Tadaki Y & Ogawa H. 1978. Plant biomass and growth increment studies in Pasoh forest. *Malayan Nature Journal* 30: 211–224.

Lu D. 2006. The potential and challenge of remote sensing-based biomass estimation. *International Journal of Remote Sensing* 27: 1297–1328.

Mazzei L, Sist P, Ruschel A, Putz FE, Marco P, Pena W & Ribeiro Ferreira E. 2010. Above-ground biomass dynamics after reduced-impact logging in the eastern Amazon. *Forest Ecology and Management* 259: 367–373.

Miettinen J & Liew SC. 2009. Estimation of biomass distribution in Peninsular Malaysia and in the islands of Sumatra, Java and Borneo based on multi-resolution remote sensing land cover analysis. *Mitigation and Adaptation Strategies for Global Change* 14: 357–373.

Patenaude G, Hill RA, Milne R, Gaveau DLA, Briggs BBJ & Dawson TP. 2004. Quantifying forest aboveground carbon content using lidar remote sensing. *Remote Sensing of Environment* 93: 368–380.

Quinones MJ & Hoekman DH. 2004. Exploration of factors limiting biomass estimation by polarimetric radar in tropical forests. *IEEE Transaction on Geosciences and Remote Sensing* 42: 86–104.

Rosenqvist A, Milne A, Lucas R, Imhoff M & Dobson C. 2003a. A review of remote sensing technology in support of the Kyoto protocol. *Environmental Science Policy* 6: 441–455.

Rosenqvist A, Shimada M, Igarashi T, Watanabe M, Tadono T & Yamamoto H. 2003b. Support to multi-national environmental conventions and terrestrial carbon cycle science by ALOS and ADEOS-II—the Kyoto and carbon initiative. *Proceedings of 2003 IEEE International on Geosciences and Remote Sensing Symposium* 3: 1471–1476.

Shimada M, Isoguchi O, Tadono T & Isono K. 2009. PLASAR radiometric calibration and geometric calibration. *IEEE Transaction on Geosciences and Remote Sensing* 3: 765–768.

Shimada M, Rosenqvist A, Watanabe M & Tadono T. 2005. The polarimetric and interferometric potential of ALOS PALSAR. In Pattier (Ed) *Proceedings in SAR Polarimetric Interferometry (POLinSAR 2005)*. 17–19 January 2005, Frascati .

Toan LT, Picard G, Martinez J, Melon P & Davidson M. 2001. On the relationships between radar measurements and forest structure and biomass. Pp 3–12 in Quegen S (Ed) *Proceedings of the Third International Symposium 'Retrieval of Bio- and Geophysical Parameters from SAR Data for Land Applications'*. 11–14 September 2001, Sheffield.

Toan LT, Quegan S, Woodward I, Lomas M, Delbart N & Picard C. 2004. Relating radar remote sensing of biomass to modeling of forest carbon budgets. *Climate Change* 76: 379–402.

Wright SJ. 2010. The future of tropical forests. *Annals of the New York Academy of Sciences* 1195: 1–27.